15th World Congress on Computational Mechanics (WCCM-XV)
8th Asian Pacific Congress on Computational Mechanics (APCOM-VIII)
Virtual Congress: 31 July – 5 August 2022
S. Koshizuka (Ed.)

CONCURRENT MULTISCALE TOPOLOGY OPTIMIZATION FOR DESIGNING DISPLACEMENT INVERTER

MUSADDIQ AL ALI[1] AND MASATOSHI SHIMODA[1]

[1] Department of Advanced Science and Technology, Toyota Technological Institute, 2-12-1 Hisakata, Tenpaku-ku, Nagoya, Aichi 468-8511, Japan
Email: alali@toyota-ti.ac.jp

Key words: Topology optimization, concurrent multiscale optimization, displacement inverter, periodic microstructure. compliant mechanism.

Abstract. *Structural light-weighting is vital for increasing energy efficiency and reducing CO_2 emissions. One of the mechanical structures that are used in numerous applications and can utilize light weighting is the displacement inverter. The displacement inverter is producing a mechanical reaction as the reverse of the input actuating action. In this research, multiscale topology optimization of compliance mechanism is used to design a lightweight displacement inverter. In this research, a hybrid topology optimization of SIMP for macroscale and ESO for microscale was used to obtain porous displacement inverter designs. Several numerical examples were investigated, and an experimental case was conducted by printing the design displacement model using 3d printer.*

1 INTRODUCTION

A compliant mechanism is a unique type of hingeless mechanism that achieves movement by relying on the elastic deformation of the entire or a portion of the mechanism itself. Compliant mechanisms are gaining popularity in the sectors of micro-electro-mechanical systems, medical devices, and aerospace due to their low noise, high precision, and lack of lubrication. The displacement inverter is one of the practical uses of the compliant mechanism. As the input actuating action is reversed, the displacement inverter produces a mechanical reaction. A lightweight displacement inverter is designed using multiscale topology optimization of compliance mechanisms in this study.

Topology optimization is presented as one of the rapidly advancing methodologies for achieving innovative designs in many applications and various physical aspects[1][2][3][4]. Associated with additive manufacturing topologically optimized structures increasingly find the way in industrial applications to produce lightweight structures with high functionality. Therefore, the goal of structural topology optimization is to discover the best and robust material distribution to maximize structural performance to weight ratio while meeting various design conditions. The homogenization method was one of the first continuum topology optimization methods for constructing compliant systems[5]. By introducing a material density function in each discretized element, which is composed of an infinite number of randomly dispersed holes, this approach transforms computationally costly structural topology optimization into efficient multiscale optimization problems. The mechanical effective characteristics of materials are determined using the homogenization theory. There are two types of ways for introducing microstructures: methods based on rank laminate composites and methods based on microcells with internal voids. For the former, the homogenization equation can be solved analytically, whereas, for the latter, numerical methods are frequently used to solve the homogenization problem. The homogenization method has the advantage of being able to put mathematical bounds on theoretical structural performance[6]. Ananthasuresh et al [7] has extended the homogenization methodology to the design of compliant mechanisms. However, the results appear to be a mean compliance design rather than a compliant mechanism design because the resulting mechanisms are not flexible enough. As a result, Nishiwaki et al. [8] developed a homogenization-based topology optimization method for the design of compliant mechanisms that includes flexibility. This method developed a multi-objective function using mutual mean compliance to successfully describe the flexibility. As the direct derivative of homogenization method, SIMP (solid isotropic microstructure with penalization) has been utilized for designing compliant mechanisms [9][10][11][12]. Moreover, the evolutionary structural optimization (ESO) approach was created on the simple premise of gradually reducing inefficient material from a structure in order to achieve the best structure possible. The basic philosophy behind ESO is the direct removal of the so-called “inefficient material” which is leading to structure to form the optimal design. It is firstly introduced by Min and Steven [13]. The cost function sensitivity is used to update the decision variables [14][15]. Updating is depending on the element sensitivity number obtained by differentiating the objective function such that of solid elements and soft elements is equal to the elemental sensitivity and zero, respectively. And As for SIMP, ESO was investigated for designing compliant mechanisms [16][17][18][19]. Furthermore, there are several methodologies that has

been used in topology optimization such as Level set [20][21][22][23][14], H^1 gradient [24][25], mesh morphing [26] ,and Phase field method [27]. The multiscale compliant mechanism has gained little attention from researchers due to the difficulty of attaining robust designs. Moreover, the grayscale nature of such problem when it is optimized using the SIMP method is limiting significantly attaining extrema due to the fluctuating effective properties for the grayscale elements at the beginning of the optimization process. The research of Sivapuram et al [28] tried to overcome such problem by using level set method to successfully design compliant mechanism. The binarized nature of the used zero level set method eased the attaining a robust design. Since this work, the multiscale concurrent optimization of compliant mechanism has not investigated. Moreover, hybrid method of SIMP and ESO has not implemented for concurrently design extreme lightweight multiscale compliant mechanism with microscale. As such, in this research, hybrid design methods of SIMP for macroscale and ESO for designing microscale is implemented in order to design porous displacement inverter. As a result, the effective properties obtained using the homogenization for the microstructure are evaluated with a dedicated finite element model, while the macrostructure's effective properties are calculated using a different finite element model. The adjoint approach is used to implement the sensitivity analysis efficiently for the concurrent design function in this study, which reduces the computational cost significantly. This paper is organized as the following: Section 2 is dedicated to the mathematical modelling of the multiscale problem. Section 3 is dedicated to presenting and discussing the numerical examples and finally, section 4 is dedicated to the conclusions.

2 EFFECTIVE ELASTICITY TENSOR AND MECHANICAL COMPLIANCE DERIVATIVE FOR MULTISCALE

Concurrent topology optimization was performed inasmuch as macro and microsystems are simultaneously optimizing the objective function on both, the micro $\boldsymbol{\rho}_{\mathrm{M}}$ and macroscale $\boldsymbol{\rho}_{\mathrm{m}}$. Macro and microscale design domains are discretized using two distinctive finite element systems. In this paper, we used bilinear structured mesh for both systems. When $\boldsymbol{\rho}$ is equal to 1, this means that the corresponding element is a solid while if it is zero, it means that the element is representing a void, as shown in Equation (1).

$$\boldsymbol{\rho}_{\mathrm{M}}, \boldsymbol{\rho}_{\mathrm{m}} = \begin{cases} 1 & \textit{Design material} \\ 0 & \textit{Void} \end{cases} \tag{1}$$

Concurrent design of multiscale problems necessitates the employment of a homogenization approach for two reasons. The first is to calculate the macrostructure's effective properties. The second goal is to apply inverse homogenization to create the microstructure and macrostructure simultaneously.

Let’s start the investigation for the evaluation of the effective elastic tensor, and starting from the assumption that using homogenization approach, Hooks law in tensor for 2D problem is taking the tensor form shown in Equation (2)

$$\begin{Bmatrix} \sigma_x \\ \sigma_y \\ \tau_{xy} \end{Bmatrix} = \begin{bmatrix} E_{11} & E_{12} & E_{14} \\ E_{21} & E_{22} & E_{23} \\ E_{31} & E_{32} & E_{33} \end{bmatrix} \begin{Bmatrix} \varepsilon_x \\ \varepsilon_y \\ \varepsilon_{xy} \end{Bmatrix} \tag{2}$$

To calculate effective elastic tensor $\mathbf{E}^{\mathrm{H}}_{ijkl}$ of the RVE of a volume V Equation (3) is used:

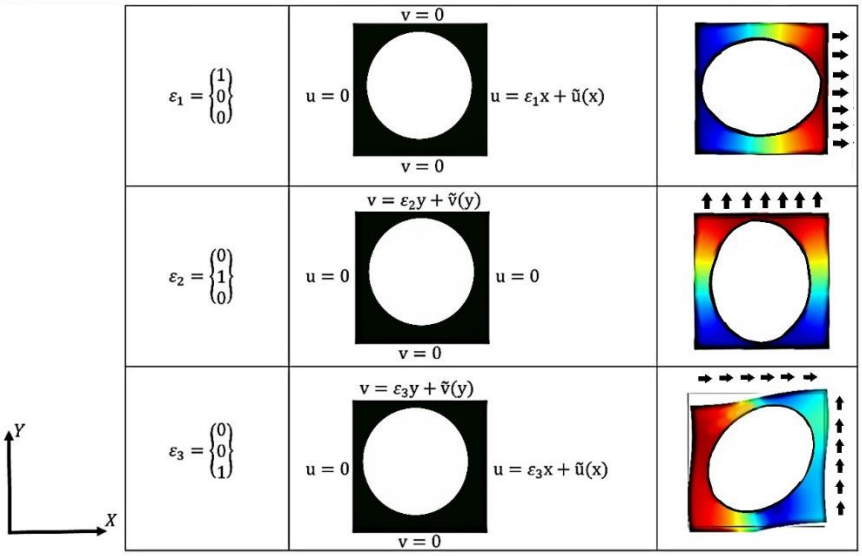

Figure 1: The three mechanical deformation modes of 2D RVE

$$\mathbf{E}^{\mathrm{H}} = \frac{1}{|V|}\int_V \mathbf{E}_{ijqp}\left(\boldsymbol{\varepsilon}^{0(kl)}_{qp} - \boldsymbol{\varepsilon}^{*(kl)}_{qp}\right)dV \tag{3}$$

Where $\mathbf{E}_{ijqp}$ is the elastic tensor of the composite materials that consisting the RVE, $\boldsymbol{\varepsilon}^{0(kl)}_{qp}$ is the linearly independent unit strain test (as shown in figure 1). $\boldsymbol{\varepsilon}^{*(kl)}_{qp}$ is periodic characteristic strain which is obtained by solving Equation (4)

$$\int_{\Omega_m} \mathbf{E}_{ijqp}\boldsymbol{\varepsilon}^{*(kl)}_{qp}\partial\gamma_n dV = \int_{\Omega_m} \mathbf{E}_{ijqp}\boldsymbol{\varepsilon}^{0(kl)}_{qp}\partial\gamma_n dV \tag{4}$$

Where $\partial\gamma_n$ is the arbitrary virtual displacement associated with unit strain case. Equation (3) is solved for the three cases of *kl*=11, 22, 12 respectively within Equation (4) (As shown in figure 1). Returning to macroscale of the problem; the structure compliance in terms of the micro and macro design variables ($\boldsymbol{\rho}_{\mathrm{M}}$ and $\boldsymbol{\rho}_{\mathrm{m}}$ respectively) is given by

$$C_{mech}\left(\boldsymbol{\rho}_{\mathrm{M}}, \mathrm{x}_{\mathrm{m}}\right)=\frac{1}{2}\sum_{i=1}^{N}\mathbf{U}_i^T\mathbf{K}_i\left(\boldsymbol{\rho}_{\mathrm{M}}, \boldsymbol{\rho}_{\mathrm{m}}\right)\mathbf{U}_i \tag{5}$$

Where $\mathbf{U}_{\mathrm{i}}$ and $\mathbf{K}_{\mathrm{i}}$ represents the nodal displacement, and the stiffness matrix of the i^{th} element with respect to the macrostructure of the total number of the element equal to *N*. The general form of the elemental stiffness matrix is taking the form:

$$\mathbf{K}=\int_V \mathbf{B}^T\mathbf{E}\mathbf{B}dV \tag{6}$$

Where $\mathbf{B}$ is the strain displacement matrix, and $\mathbf{E}$ is the elastic tensor of the element. For microstructure case, the elastic tensor $\mathbf{E}_{micro}$ is formulated to comply with the SIMP interpolation scheme such that, the penalized design variable $\boldsymbol{\rho}_{\mathrm{m}}$ to power ($p=3$) [29] is associated with the elastic tensor of the based material $\mathbf{E}_0$ such that:

$$\mathbf{E}^{\mathrm{H}}=\boldsymbol{\rho}_{\mathrm{m}}{}^{3}\mathbf{E}_0 \tag{7}$$

The associated effective elastic tensor of the microstructure $\mathbf{E}^{\mathrm{H}}$, which is calculated using homogenization method, is used to establish the elemental elastic tensor of the macroscale $\mathbf{E}_{macro}$ with similar material interpolation scheme as for the microstructure system.

$$\mathbf{E}_{macro}=\boldsymbol{\rho}_{\mathrm{m}}^{3}\mathbf{E}^{\mathrm{H}} \tag{8}$$

The generalized model of mechanically activated compliant mechanism problem is linearly implemented by assuming the actuator with in linear strain limits, subjected to spring of stiffness K_{in} and a force F_{in} at the input point A. The objective function is maximizing the displacement at the output point B.

$$\begin{aligned}&\max_{\boldsymbol{\rho}}:\ \mathbf{U}_{out}\\ &\text{s.t.}\begin{cases}\mathbf{K}\mathbf{U}=\mathbf{F}\\ \int_{\Omega_{dM}}\boldsymbol{\rho}\,d\boldsymbol{\rho}\le v\ ,\ \boldsymbol{\rho}\in(0,1] \quad \forall\boldsymbol{\rho}\in\Omega\end{cases}\end{aligned} \tag{9}$$

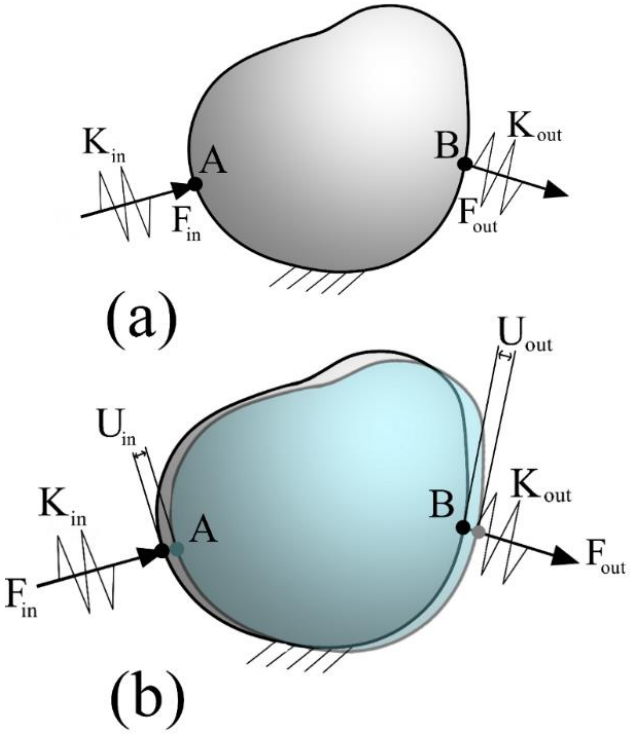

Figure 2: Compliant mechanism design problem

$$
\begin{aligned}
&\textit{find} \quad \boldsymbol{\rho}_{\mathrm{M}}, \boldsymbol{\rho}_{\mathrm{m}} \quad (\mathrm{M}=1,2,..,N_{\mathrm{M}}\,;\mathrm{m}=1,2,..,N_{\mathrm{m}}) \\
&\max_{\boldsymbol{\rho}_{\mathrm{M}},\boldsymbol{\rho}_{\mathrm{m}}}: \ \mathbf{U}_{out} \\
&\text{s.t.} \begin{cases} \mathbf{K}\left(\boldsymbol{\rho}_{\mathrm{M}}, \boldsymbol{\rho}_{\mathrm{m}}\right)\mathbf{U}=\mathbf{F} \\ \\ \displaystyle\int_{\Omega_{dM}} \boldsymbol{\rho}_{\mathrm{M}} d\boldsymbol{\rho}_{\mathrm{M}} \le v_{\mathrm{M}} \ , \ \boldsymbol{\rho}_{\mathrm{M}} \in (0,1] \quad \forall \boldsymbol{\rho}_{\mathrm{M}} \in \Omega_{dM} \\ \\ \displaystyle\int_{\Omega_{dm}} \boldsymbol{\rho}_{\mathrm{m}} d\boldsymbol{\rho}_{\mathrm{m}} \le v_{\mathrm{m}} \ , \ \boldsymbol{\rho}_{\mathrm{M}} \in (0,1] \quad \forall \boldsymbol{\rho}_{\mathrm{m}} \in \Omega_{dm} \end{cases}
\end{aligned}
\tag{10}
$$

Here, N_{M} , and N_{m} are the element number of the macro- and the microscale structure respectively. v_{M} and v_{m} are the volume fraction of the design variable $\boldsymbol{\rho}_{\mathrm{M}}$ and $\boldsymbol{\rho}_{\mathrm{m}}$ within the macro and micro design domains (Ω_{dM} and Ω_{dm} respectively).

2.2 Sensitivity analysis and optimization method

Taking into consideration that in our linear analysis, the mechanical loading vector **F** is design independent, the sensitivity analysis is given in equation 11

$$\frac{\partial \mathbf{U}_{out}}{\partial \boldsymbol{\rho}} = \mathbf{U}_{in}^{T} \frac{\partial \mathbf{K}}{\partial \boldsymbol{\rho}} \mathbf{U}_{out} \tag{11}$$

while $\frac{\partial \mathbf{K}}{\partial \boldsymbol{\rho}}$ in term of macroscale is

$$\frac{\partial \mathbf{K}}{\partial \boldsymbol{\rho}_{\mathrm{M}}} = \int_{|\Omega_{\mathrm{M}}|} \mathbf{B}^{T} \frac{\partial \mathbf{E}^{\mathrm{H}}(\boldsymbol{\rho}_{\mathrm{M}})}{\partial \boldsymbol{\rho}_{\mathrm{M}}} \mathbf{B}\, d\Omega_{\mathrm{M}} \tag{12}$$

And in term of microscale design variable

$$\frac{\partial \mathbf{K}}{\partial \boldsymbol{\rho}_{\mathrm{m}}} = \int_{|\Omega_{\mathrm{m}}|} \mathbf{B}^{T} \frac{\partial \mathbf{E}^{\mathrm{H}}(\boldsymbol{\rho}_{\mathrm{m}})}{\partial \boldsymbol{\rho}_{\mathrm{m}}} \mathbf{B}\, d\Omega_{\mathrm{m}} \tag{13}$$

The derivative of the homogenized material's elastic tensor with respect to micro design variable $\frac{\partial \mathbf{E}^{\mathrm{H}}(\boldsymbol{\rho}_{\mathrm{m}})}{\partial \boldsymbol{\rho}_{\mathrm{m}}}$ is:

$$\frac{\partial \mathbf{E}^{\mathrm{H}}(\boldsymbol{\rho}_{\mathrm{m}})}{\partial \boldsymbol{\rho}_{\mathrm{m}}} = \frac{p}{|\Omega_{\mathrm{m}}|} \int_{\Omega_{\mathrm{m}}} \left(\boldsymbol{\rho}_{\mathrm{m}}^{p-1}\right) \mathbf{E}_{ijqp}^{0} \left(\boldsymbol{\varepsilon}_{qp}^{0(kl)} - \boldsymbol{\varepsilon}_{qp}^{*(kl)}\right) d\Omega_{\mathrm{m}} \tag{14}$$

The optimization method used in this work is the SIMP method for optimizing the macrostructure and the ESO method for optimizing the microstructure. This hybrid form of optimizing allowed the attaining of good designs as well as lowering the computational cost significantly. Furthermore, optimality criteria method is used to update the design variables. To guarantee that solutions to the topology optimization problem exist and that checkerboard problem do not arise, a sensitivity filter is introduced to modify the sensitivities $\dot{C}\ (\mathbf{x}_{\mathrm{M}})$ and $\dot{C}\ (\mathbf{x}_{\mathrm{m}})$ as follows:

$$\hat{\dot{C}} = \frac{\partial C}{\partial \mathbf{x}_e} = \frac{1}{\mathbf{x}_e \sum_{f=1}^{N} H_f} \sum_{f=1}^{N} H_f \mathbf{x}_f \frac{\partial C}{\partial \mathbf{x}_f} \tag{15}$$

Where H_f is the convolution operator to perform the modification, $\mathbf{x}_e$ is the design variable at which the sensitivity is calculated, and $\mathbf{x}_f$. The H_f is defined as

$$H_f = r - dist(e, f),\ \{f \in N \,|\, dist(e, f) \le r\} \tag{16}$$

After modifying the sensitivity, the following is a heuristic updating technique:

$$\mathbf{x}_e^{updated} = \begin{cases} \max(0, \mathbf{x}_e - \varepsilon) & if \ \ \mathbf{x}_e B_e^{\omega} \le \max(0, \mathbf{x}_e - \varepsilon) \\ \max(0, \mathbf{x}_e + \varepsilon) & if \ \ \mathbf{x}_e B_e^{\omega} \ge \max(1, \mathbf{x}_e - \varepsilon) \\ \mathbf{x}_e B_e^{\omega} & Otherwise \end{cases} \quad (17)$$

where ε denotes a positive search step. Moreover, ω which is equal to 1/2 denotes a numerical damping coefficient, and B_e denotes the optimality condition:

$$B_e = -\frac{\partial C}{\partial \mathbf{x}_e} \Big/ L \frac{\partial V}{\partial \mathbf{x}_e} \quad (18)$$

Where L here is a Lagrangian multiplier, and $\frac{\partial V}{\partial \mathbf{x}_e}$ is the volumetric topological derivative. The general algorithm for concurrent multiscale and hybrid topology optimization for displacement inverter is illustrated in figure 3.

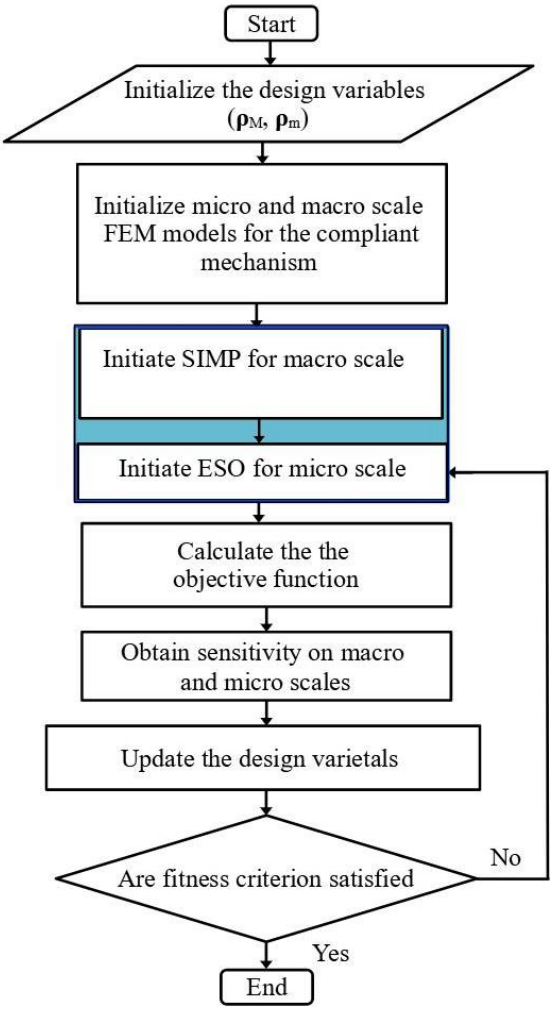

Figure 3: Flowchart of concurrent multiscale displacement inverter optimization

3 NUMERICAL INVESTIGATIONS

3.1 Concurrent multiscale displacement inverter designs

In this section, we are investigating several examples of displacement inverters. The first model is having 150 and 200 mm in the x and the y directions (As shown in Figure 4 (a)). The multiscale design is shown in Figures 4 (b), (c), and (d). As shown in Figures 5 (a) and (b) the microscale is recirculating the stored strain energy inside it in order to distribute it on the macroscale as a response to the applied force to give the prescribed and desired displacement reaction. Furthermore, two other cases are investigated (i.e., cases (e) and (i) in Figure 4).

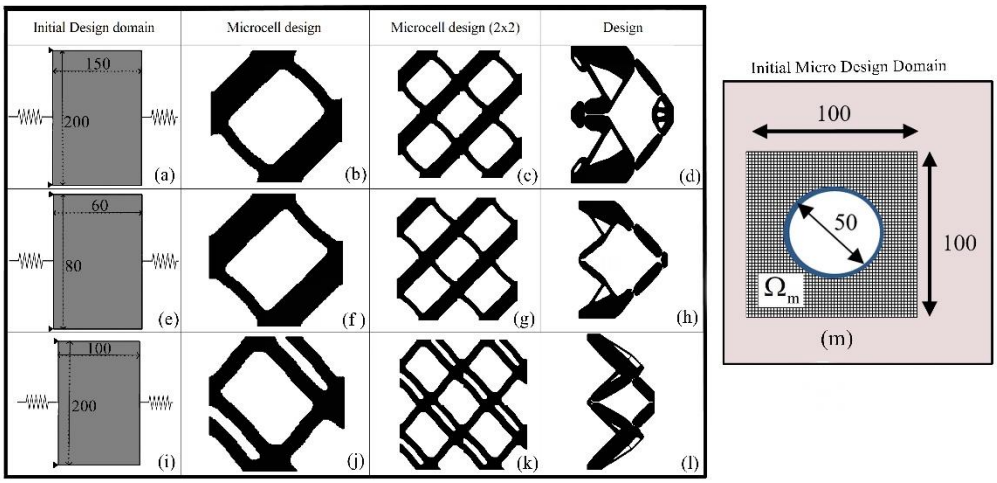

Figure 4: Designs domain and the macro and microscale designs

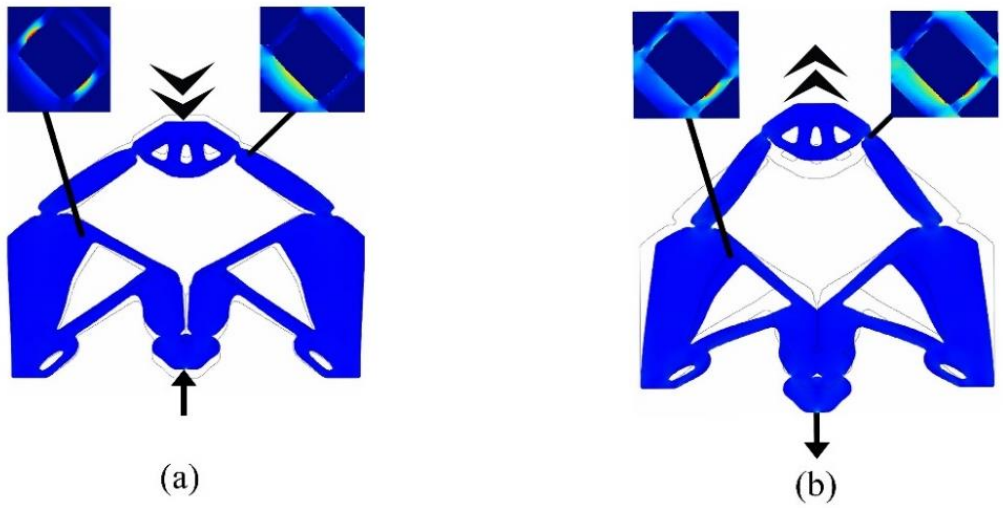

Figure 5: Concurrent multiscale design of displacement inverter (a) under compression (b) under tension

3.2 Experimental study

To verify the design of our concurrent multiscale hybrid topology optimization of the porous displacement inverter, a printed model of the first case that is shown in Figure 4 (a) is prepared. The material used was an Acrylonitrile Butadiene Styrene (ABS). The model was prepared using Stratasys F170 3D printer. Figure 6 presents the prepared specimen under testing displacement. As shown in figure 6, by inserting a displacement (-Δ) from the top, the lower point is moving with (Δ) upward.

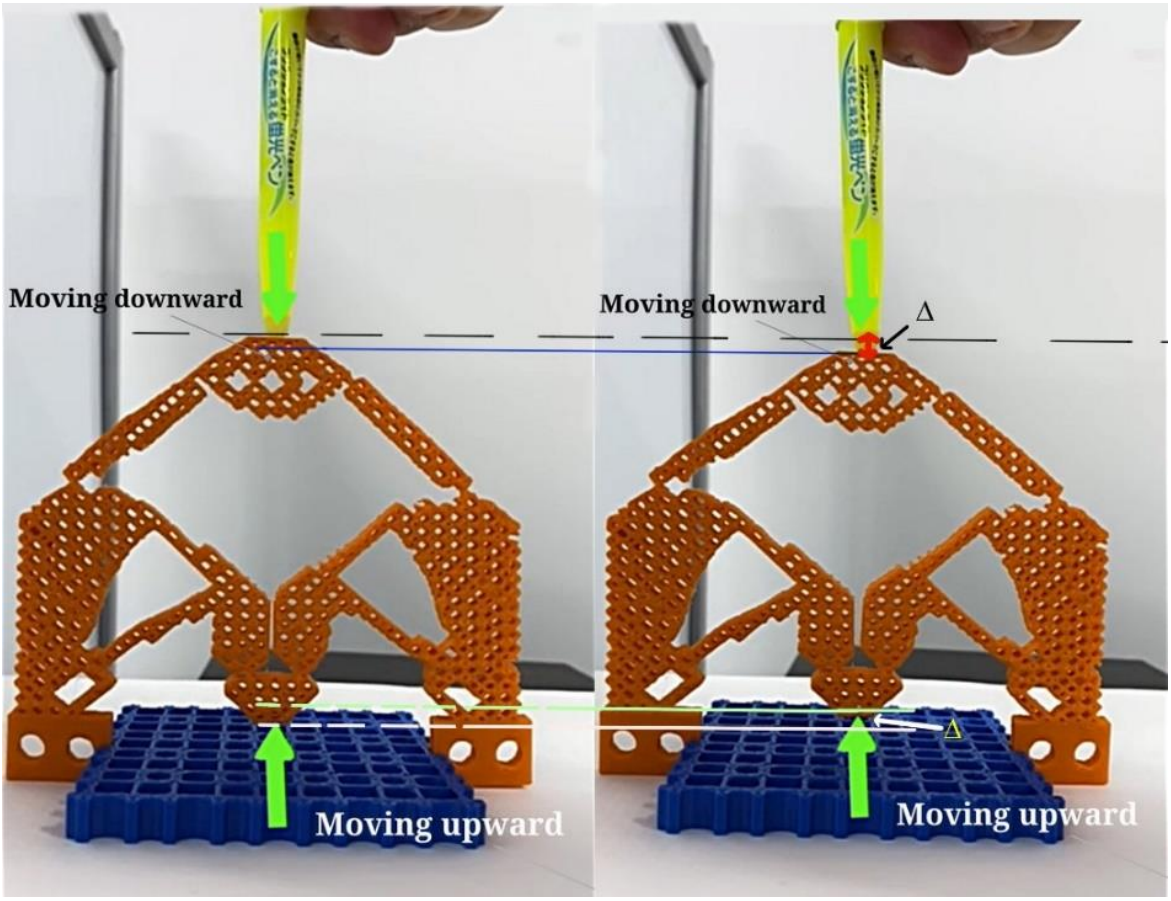

Figure 6: The 3D printed concurrent multiscale design of displacement inverter

4 CONCLUSIONS

The numerical examples showed a good design response of the microscale design with the spatial configuration and the boundary condition of the design domain on both macro and microstructure. Furthermore, this study found that by addressing microscale design with the concurrent optimization process, it is possible to get a desirable spatial configuration of materials while reducing weight. the spatial arrangements for the various scenarios revealed an elaboration for distributing strain energy in the most efficient manner possible in relation to macrostructure design. Our hybrid form of concurrently utilizing SIMP for designing

macroscale and ESO for designing microscale allowed the attaining of good designs as well as lowering the computational cost significantly. As a result, the proposed design process has the potential to produce durable and new lightweight and porous displacement inverters' designs with unique and high adaptability of elastic properties. Moreover, the concurrent multiscale design is verified experimentally.

REFERENCES

[1] M. Al Alia, A.Y. Sahibb, M. Al Alic, Teeth implant design using weighted sum multi-objective function for topology optimization and real coding genetic algorithm, in: 6th IIAE Int. Conf. Ind. Appl. Eng. 2018, The Institute of Industrial Applications Engineers, Japan, 2018: pp. 182–188. https://doi.org/10.12792/iciae2018.037.

[2] M.A. Al-Ali, M.A. Al-Ali, A. Takezawa, M. Kitamura, Topology optimization and fatigue analysis of temporomandibular joint prosthesis, World J. Mech. (2017) **7:**323–339.

[3] R.S. Abass, M. Al Ali, M. Al Ali, Shape And Topology Optimization Design For Total Hip Joint Implant, in: World Congr. Eng. 2019, 2019.

[4] M. Al Ali, M. Al Ali, A.Y. Sahib, R.S. Abbas, Design micro piezoelectric actuated gripper for medical applications, in: Proc. 6th IIAE Int. Conf. Ind. Appl. Eng. Japan, 2018: pp. 175–180.

[5] M.P. Bendsøe, N. Kikuchi, Generating optimal topologies in structural design using a homogenization method, Comput. Methods Appl. Mech. Eng. 71 (1988) 197–224.

[6] B. Hassani, E. Hinton, A review of homogenization and topology optimization I—homogenization theory for media with periodic structure, Comput. & Struct. (1998) **69:**707–717.

[7] G.K. Ananthasuresh, S. Kota, Y. Gianchandani, Systematic synthesis of microcompliant mechanisms-preliminary results, in: Proc. 3rd Natl. Conf. Appl. Mech. Robot, 1993.

[8] S. Nishiwaki, M.I. Frecker, S. Min, N. Kikuchi, Topology optimization of compliant mechanisms using the homogenization method, Int. J. Numer. Methods Eng. (1998) **42:** 535–559.

[9] O. Sigmund, On the design of compliant mechanisms using topology optimization, J. Struct. Mech. (1997) **25:**493–524.

[10] O. Sigmund, S. Torquato, Design of smart composite materials using topology optimization, Smart Mater. Struct. (1999) **8:** 365–379.

[11] J. Huang, W. Ge, F. Yang, Topology Optimization of the Compliant Mechanism for Shape Change of Airfoil Leading Edge, ACTA Aeronaut. Astronaut. Sin. (2016) **37:**989-992.

[12] K. Maute, D.M. Frangopol, Reliability-based design of MEMS mechanisms by topology optimization, Comput. & Struct. (2003) **81:**813–824.

[13] Y.M. Xie, G.P. Steven, A simple evolutionary procedure for structural optimization, Comput. & Struct. (1993) **49:**885–896.

[14] M. Al Ali, M. Shimoda, Investigation of concurrent multiscale topology optimization for designing lightweight macrostructure with high thermal conductivity, Int. J. Therm.

Sci. (2022) **179:**107653. https://doi.org/https://doi.org/10.1016/j.ijthermalsci.2022.107653.
[15] M. Zhou, G.I.N. Rozvany, On the validity of ESO type methods in topology optimization, Struct. Multidiscip. Optim. (2001) **21:**80–83.
[16] R. Ansola, E. Veguer\'\ia, J. Canales, J.A. Tárrago, A simple evolutionary topology optimization procedure for compliant mechanism design, Finite Elem. Anal. Des. (2007) **44:**53–62.
[17] X. Huang, Y.M. Xie, Evolutionary topology optimization of continuum structures with an additional displacement constraint, Struct. Multidiscip. Optim. (2010) **40:**409–416.
[18] M.G. Im, J.Y. Park, S.Y. Han, others, A New Topology Optimization Scheme Based on BESO for Electro-thermal-compliant Mechanisms, in: Proc. 6th Australas. Congr. Appl. Mech., 2010: pp. 159–168.
[19] R. Ansola, E. Veguer\'\ia, A. Maturana, J. Canales, 3D compliant mechanisms synthesis by a finite element addition procedure, Finite Elem. Anal. Des. (2010) **46:**760–769.
[20] M. Al Ali, Toward fully autonomous structure design based on topology optimization and image processing, in: Proc. 6th IIAE Int. Conf. Intell. Syst. Image Process., The Institute of Industrial Applications Engineers, 2018.
[21] M. Al Ali, Design offshore spherical tank support using shape optimization, in: Proc. 6th IIAE Int. Conf. Intell. Syst. Image Process., 2018.
[22] M. Al Ali, M. Al Ali, R.S. Saleh, A.Y. Sahib, Fatigue Life Extending For Temporomandibular Plate Using Non Parametric Cascade Optimization, in: Proc. World Congr. Eng. 2019, 2019: pp. 547–553.
[23] J.A. Sethian, A. Wiegmann, Structural boundary design via level set and immersed interface methods, J. Comput. Phys. (2000) **163:**489–528.
[24] M. Fujioka, M. Shimoda, M. Al Ali, Shape optimization of periodic-microstructures for stiffness maximization of a macrostructure, Compos. Struct. (2021) 113873.
[25] M. Al Ali, A. Takezawa, M. Kitamura, Comparative Study of Stress Minimization Using Topology Optimization and Morphing Based Shape Optimization Comparative Study of Stress Minimization Using Topology Optimization and Morphing Based Shape Optimization, in: Asian Congr. Struct. Multidiscip. Optim., 2018.
[26] M. Burger, R. Stainko, Phase-field relaxation of topology optimization with local stress constraints, SIAM J. Control Optim. (2006) **45:**1447–1466.
[27] R. Sivapuram, P.D. Dunning, H.A. Kim, Simultaneous material and structural optimization by multiscale topology optimization, Struct. Multidiscip. Optim. (2016) **54:**1267–1281.
[28] M.P. Bendsøe, Optimal shape design as a material distribution problem, Struct. Optim. (1989) **1:**193–202.